High-Resolution Structure of the Extracellular Aspartic Proteinase from *Candida tropicalis* Yeast[†]

Jindrich Symersky,[‡] Michel Monod,[§] and Stephen I. Foundling*,[||]

Laboratory of Protein Crystallography, Crystallography Research Program, Oklahoma Medical Research Foundation, 825 N.E. 13th Street, Oklahoma City, Oklahoma 73104, Center for Macromolecular Crystallography, University of Alabama, 1918 University Boulevard, Birmingham, Alabama 35294, and Laboratorie de Mycologie, Service de Dermatologie, Centre Hospitalier, University Vaudois, 1011 Lausanne, Switzerland

Received March 17, 1997; Revised Manuscript Received June 18, 1997[⊗]

ABSTRACT: The crystal structure of the secreted aspartic proteinase from *Candida tropicalis* yeast (SAPT) has been determined to 1.8 Å resolution. The classic aspartic proteinase bilobal structure and domain topology is conserved in SAPT, with the substrate binding cleft situated between the two domains. Structural comparisons made with pepsin indicate that insertions and deletions in the primary sequence modify the SAPT structure to create a more spacious substrate binding cleft with altered specificity. An unexpected tetrapeptide has been found to occupy binding sites $S_1'-S_3'$, and this suggests the order of release of peptide products in the catalytic mechanism of these enzymes. Structural features are considered with regard to previous substrate specificity data.

Opportunistic infections caused by *Candida* yeasts are becoming one of the major health threats for long term survival of immune-compromised patients (DuPont *et al.,* 1994; Odds, 1994; Swartz, 1994). Yeasts of the genus *Candida*, which include the strains of the species *Candida albicans*, *Candida tropicalis*, and *Candida parapsilosis*, secrete highly active aspartic proteinases (SAP). A direct correlation exists between the virulence of these yeasts and the secretion of the aspartic proteinases (Cutler, 1991); consequently, these enzymes are becoming attractive targets for therapeutic drug design. Inhibition of these enzymes may provide a way to block the invasive proteolytic stages of *Candida fungemia* and allow novel treatment regimes of candidiasis to be developed. The information derived here from the crystal structure determination of the secreted aspartic proteinase from the *C. tropicalis* yeast (SAPT) may aid in understanding the structure−function characteristics of the *Candida* proteinase family, such as substrate recognition and catalytic mechanism, and eventually assist us with inhibitor design.

C. tropicalis is the predominant source of fungal infections in neutropenic cancer patients and is a common isolate in hospitals. The most widely studied *C. tropicalis* virulence attributes are "adhesins", hyphae formation, and secreted aspartic proteinases. During an infectious process, *Candida* yeast binds to and colonizes superficial sites in the form of budding yeast cells, which transform to hyphae and penetrate deeper into the host tissues. Indirect evidence implies a major role for the aspartic proteinase secreted by *C. tropicalis* in this complicated process. Studies have demonstrated SAP antigen at the surface of fungal elements in mucosal specimens (Rüchel *et al.,* 1991; Rüchel, 1992), in tissues during disseminated candidiasis (MacDonald & Odds, 1980; Ray & Payne, 1987; Rüchel *et al.,* 1988), and in macrophages after phagocytosis of yeast cells (Borg & Rüchel, 1990). Further evidence for the role of SAP in virulence is also derived from experiments where pepstatin A, a specific inhibitor of aspartic proteinases, is able to block adherence and invasion of *C. albicans* (Calderone & Stevens, 1991; Ray & Payne, 1988).

Aspartic proteinases comprise a group of enzymes, found in or are secreted by a variety of eukaryotic organisms, which demonstrate an unusually broad range of specificities. For example, the gastric pepsins (Foltmann, 1981) and chymosin (Kay *et al.,* 1981) have a physiological role in food digestion in the stomachs of many species; the lysosomal enzyme cathepsin D catalyzes intracellular proteolysis (Shewale *et al.,* 1985; Blum *et al.,* 1991), and the granular-based yeast proteinase A from *Saccharomyces cerevisiae* (Dreyer *et al.,* 1985) has a similar role in the yeast cell. A large number of fungi such as *Endothia parasitica* (Sardinas, 1965), *Rhizopus chinensis* (Subramanian, 1976), and *Penicillium janthinellum* (Hsu *et al.,* 1976) secrete aspartic proteinases into the growth media to hydrolyze proteins for nutrient requirements.

The archetypic enzyme of the aspartic proteinase family is porcine pepsin. The pepsin-like enzymes catalyze proteolysis in an acidic solution (Fruton, 1971) and have a catalytic optimum within the range of pH 2.0−pH 5.0 (Morihara, 1973; Knowles, 1970). Extensive chemical studies on pepsin led to the identification of two aspartic acid residues, Asp 32 and Asp 215 (pepsin numbering), which are essential to catalysis (Tang *et al.,* 1973; Chen *et al.,* 1972). The most recent addition to the family of aspartic proteinases are the retroviral aspartic proteinases (Wlodawer *et al.,* 1989; Debouck & Metcalf, 1990), which are responsible for processing the HIV-1 gag and gag-pol polyproteins into their respective domains during provirus maturation.

[†] This work was supported by Grant R29 3134308 (S.I.F.) from the National Institutes of Health and a New Investigators Award (S.I.F.) from the Oklahoma Center for the Advancement of Science and Technology (OCAST).

* Author to whom correspondence should be addressed.
[‡] University of Alabama.
[§] University Vaudois.
[||] Oklahoma Medical Research Foundation.

[⊗] Abstract published in *Advance ACS Abstracts,* August 15, 1997.

S0006-2960(97)00613-2 CCC: $14.00

Many mammalian and fungal aspartic proteinase structures, together with enzyme−inhibitor complexes, have been solved crystallographically during the past ten years. These structures have shown that aspartic proteinases fold almost uniformly to form bilobal molecules with extensive β-sheet secondary structure. Deletions or insertions in the primary amino acid sequences generally lead to local modifications in the secondary structure. The structures of the enzyme−inhibitor complexes have shown that the substrate binding cleft is quite extensive and can accommodate at least eight residues.

The crystallographic structures of two closely related aspartic proteinases from *C. albicans* yeast have been reported during the past twelve months. The SAP2X proteinase derived from an infectious clinical isolate of *C. albicans* was described at 2.5 Å resolution by Abad-Zapatero *et al.* (1996). The SAP2X proteinase likely represents an isoform of the SAP2 enzyme that was purified from *C. albicans* strain ATCC 10261 and has been resolved to 2.1 Å by Cutfields *et al.* (1995). The structure of the *C. tropicalis* (SAPT) enzyme we present here is related to these enzymes and is generally homologous in its overall tertiary structure but is notably different in the primary amino acid sequence.

METHODS

Crystallization. SAPT was isolated and purified as described previously (Fusek *et al.,* 1994) and concentrated in water to 30 mg/mL. Crystals were grown by the hanging drop method. A droplet of SAPT solution was equilibrated against a reservoir containing 0.1 M sodium acetate buffer and 20% ethanol at pH ∼5.0 and 20 °C. The droplets contained equal volumes of the SAPT protein stock and the reservoir solution. Long prism crystals grew within 2 weeks. The SAPT crystals were orthorhombic, space group $P2_12_12_1$, and had the following unit cell dimensions: $a = 49.96$ Å, $b = 51.43$ Å, and $c = 128.9$ Å, with one molecule per asymmetric unit. Crystals diffracted well to 1.8 Å, and weak diffraction was detectable to a nominal 1.45 Å resolution.

Autodigestion. Aspartic proteinases are commonly degraded when left in concentrated aqueous solution at room temperature. To test whether SAPT significantly autodigests under crystallization conditions, we left a concentrated sample of 15 mg/mL proteinase to stand at 20 °C for 12 h. An initial sample was taken, and then samples were withdrawn at 2 h intervals for SDS−PAGE analysis. The first SAPT sample ran as a single band with an apparent molecular mass of ∼40 kDa. After 12 h of autodigestion, two major bands appeared, one at ∼40 kDa and a second at ∼28 kDa. After 24 h, the overall number of bands had increased within the size range of 40−10 kDa, but their intensity had decreased. To reduce autodigestion, all reagents were kept on ice and proteinase was removed from −70 °C storage and immediately thawed and used in crystallizations. SDS−PAGE performed on dissolved SAPT crystals showed only one protein band at ∼40 kDa and a slight band at ∼38 kDa, indicating that the protein crystallized without significant autodigestion. Amino-terminal sequencing of dissolved SAPT crystals confirmed that the predominant species of SAPT in crystals corresponded to full length SAPT.

Data Collection. The diffraction data were collected on a Siemens X-1000 multiwire area detector with X-rays produced by a direct-drive Siemens rotating copper anode and graphite monochromator. Data collection was controlled using the program FRAMBO (Siemens, 1989). Two diffraction data sets were collected from four crystals and processed using SADIE and SAINT (Siemens, 1989). Data set 1 was at high resolution and consisted of a merged and scaled data set from three SAPT crystals. Data set 2 was collected from one crystal to verify the unexpected electron density in the active site cleft of SAPT. The data statistics are shown in Table 5.

Molecular Replacement. The programs AMoRe (Navaza, 1994) and X-PLOR (Brunger, 1992) were used for initial phasing by molecular replacement. The atomic coordinates of human cathepsin D (Metcalf & Fusek, 1993) were used as an initial search model. Consistent but poorly discriminated solutions were found with both programs. Later, we found a well-discriminated solution, using a partially refined model of *C. albicans* aspartic proteinase (Abad-Zapatero *et al.,* 1996).

Model Building and Refinement. The initial *R*-factor, calculated for the best *C. albicans* solution, was 47% within the resolution limits of 15−2.5 Å. Packing diagrams did not indicate any serious overlaps of the symmetry-generated equivalents with this solution. After positional refinement in X-PLOR and partial substitution of the SAPT sequence into the electron density map, the *R*-factor dropped to 34%. Poorly defined areas of the model, such as several loops and most of the carboxyl-terminal domain, were systematically omitted section by section in the SAPT model. These transitional models were extensively refined in X-PLOR by the simulated annealing procedure. The SAPT sequence was rebuilt into $2F_o - F_c$ and $F_o - F_c$ electron density maps prior to continuing to the next refinement step. When 95% of the SAPT sequence was fitted and the maps showed no further improvement in the flexible parts of some loops, the *R*-factor for the model was 27% within the resolution limits of 15−2.5 Å.

At this stage in refinement, we observed significant and clearly isolated electron density in the carboxyl-terminal part of the binding cleft ($S_1'-S_3'$) which then extended out of the enzyme. A tetrapeptide chain was modeled to fit this density. We continued model refinement by including higher-resolution data in small shells out to the 1.8 Å resolution limit of the data. The entire model was refined at each step by simulated annealing refinement using X-PLOR. $2F_o - F_c$ and $F_o - F_c$ difference electron density maps were calculated after each refinement step, and the model was improved using the software CHAIN (Sack, 1988). The final refined model of SAPT has 334 amino acids of the protein, and a tetrapeptide Thr-Ile-Thr-Ser is fitted to the prime part of the binding cleft. In addition, 231 water molecules and 6 ethanol molecules are occupying well-defined solvent peaks. The final *R*-factor for the SAPT model is 18.3% for the resolution shell of 8.0−1.8 Å, and $F > 2\sigma_F$. Isotropic temperature factors of the non-hydrogen atoms were refined separately. The refinement statistics are summarized in Table 5. The electron density defining SAPT is poor in four loop regions. These regions of disorder correspond to the loops at positions 51−53, 135 and 136, 245 and 246, and 283−285, respectively (SAPT numbering).

The SAPT structure has been fully analyzed using the PROCHECK software (Laskowski *et al.,* 1993). Coordinates

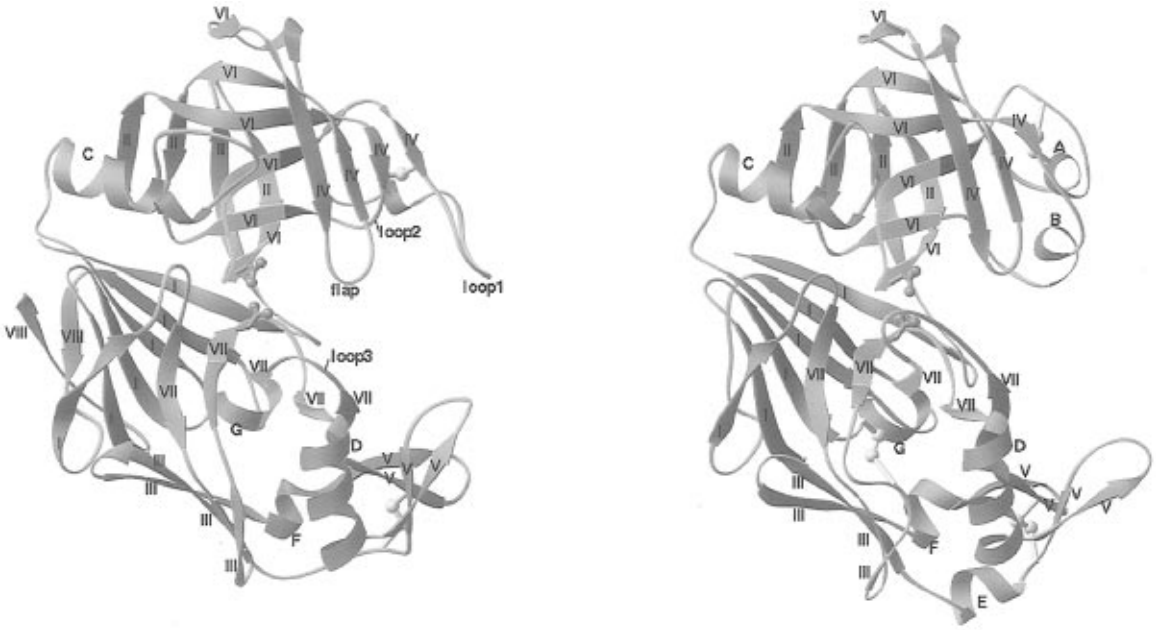

FIGURE 1: Comparison of the folding and secondary structure between SAPT (left image) and porcine pepsin (right image). Roman numerals I−VIII indicate strands of β-sheet. Letters A−G indicate helices. ψ-Motifs are highlighted in magenta, catalytic aspartates in red, and disulfide bridges in yellow. The picture was rendered using the RIBBONS program (Carson, 1995).

have been deposited in the Brookhaven Protein Data Bank under the acquisition number 1PCT.

RESULTS

C. tropicalis Molecular Structure. The SAPT enzyme shares the archetypic fold and overall topology of the classic aspartic proteinases (Davies, 1990). Two similar domains composed predominantly of β-sheet form the bilobal enzyme which is divided by a large substrate binding cleft. Each domain contributes one aspartic acid to the catalytic pair which is situated at the center of the binding cleft. The catalytic pair is shielded from solvent by a conserved β-hairpin loop, consisting of residues Asp 79−Gln 91 known as the "flap".

The structure of pepsin, which is well-established through independent determination by several groups (Abad-Zapatero *et al.*, 1990; Andreeva *et al.*, 1978; Cooper *et al.*, 1990; Sielecki *et al.*, 1990), was used to demonstrate the similarities and differences in SAPT secondary structure and overall topology (Figure 1). The structure-based comparative sequence alignment between pepsin and SAPT with overlaid elements of secondary structure is shown in Figure 2.

In our model of SAPT, there are five residues which differ with respect to the published sequence (Togni *et al.*, 1991). The identification of these was based upon interpretation of electron density maps in combination with resequencing (M. Monod, personal communication). The changes are V131 → D, S139 → D, C158 → L, D159 → Y, and V262 → F.

Seven β-sheets have been recognized in pepsin and described in terms of layered sheets with approximate orthogonal packing of strands between adjacent layers (Sielecki *et al.*, 1990; Chothia & Janin, 1982). This arrangement of β-sheets results in globular domains with an extensive hydrophobic core. Sheet I forms an interdomain base of the molecule. The amino-terminal domain is made of three layers of sheets II, IV, and VI, respectively. The carboxyl-terminal domain has two layers of sheets III and VII, and a separate sheet V. SAPT conserves this pattern of β-structure with some small variations. Sheet IV of the amino-terminal domain has an added β-strand A45−C47. The carboxyl-terminal domain of SAPT has two additional short β-strands, G174−D176 and I331−A333 labeled as a separate sheet VIII in Figures 1 and 2.

Seven small helices have been described in the pepsin structure. Helices C, D, F, and G are conserved in SAPT, while short helices A, B, and E are absent. The helical turn F58−K60 in SAPT probably corresponds to pepsin helix A; however, there is a weaker structural homology in this region. Pepsin helical turns P58−D60 and P126−I128 are also conserved in the SAPT structure.

Although much of the secondary structure is conserved between pepsin and SAPT, there are three noticeable differences which may influence the substrate specificity of SAPT. The first is at residues 43−63 where SAPT lacks helix A and has an additional strand, β-sheet IV. Also, an insertion of 11 amino acids between cysteine 47 and 59 results in an extended flexible loop (loop 1) which resembles a second flap, which differs from the classic flap of the typical aspartic proteinases by not having well-defined secondary structure and extending further into the solvent region. The second difference in SAPT is the deletion between S118 and V119 (loop 2), which is a short helix B in pepsin positioned at the boundary between the S_5 and S_3 binding pockets [nomenclature of binding cleft taken from Schechter and Berger (1970)]. This deletion is likely to influence substrate binding in SAPT. The third significant difference in SAPT is the deletion between D295 and A296 (loop 3); this is similar to the fungal enzymes rhizopuspepsin, endothiapepsin, and penicillopepsin.

The insertion of loop 1 and the deletion of helix B, to fashion loop 2, make SAPT distinct from the classic fungal enzymes, all of which are more similar to pepsin at these positions. The net effect of these changes creates a wider binding cleft in SAPT, particularly in the nonprimed side of the cleft at subsites S_3 and S_5, and is shown in Figure 3. The wider binding cleft in SAPT may correlate with the

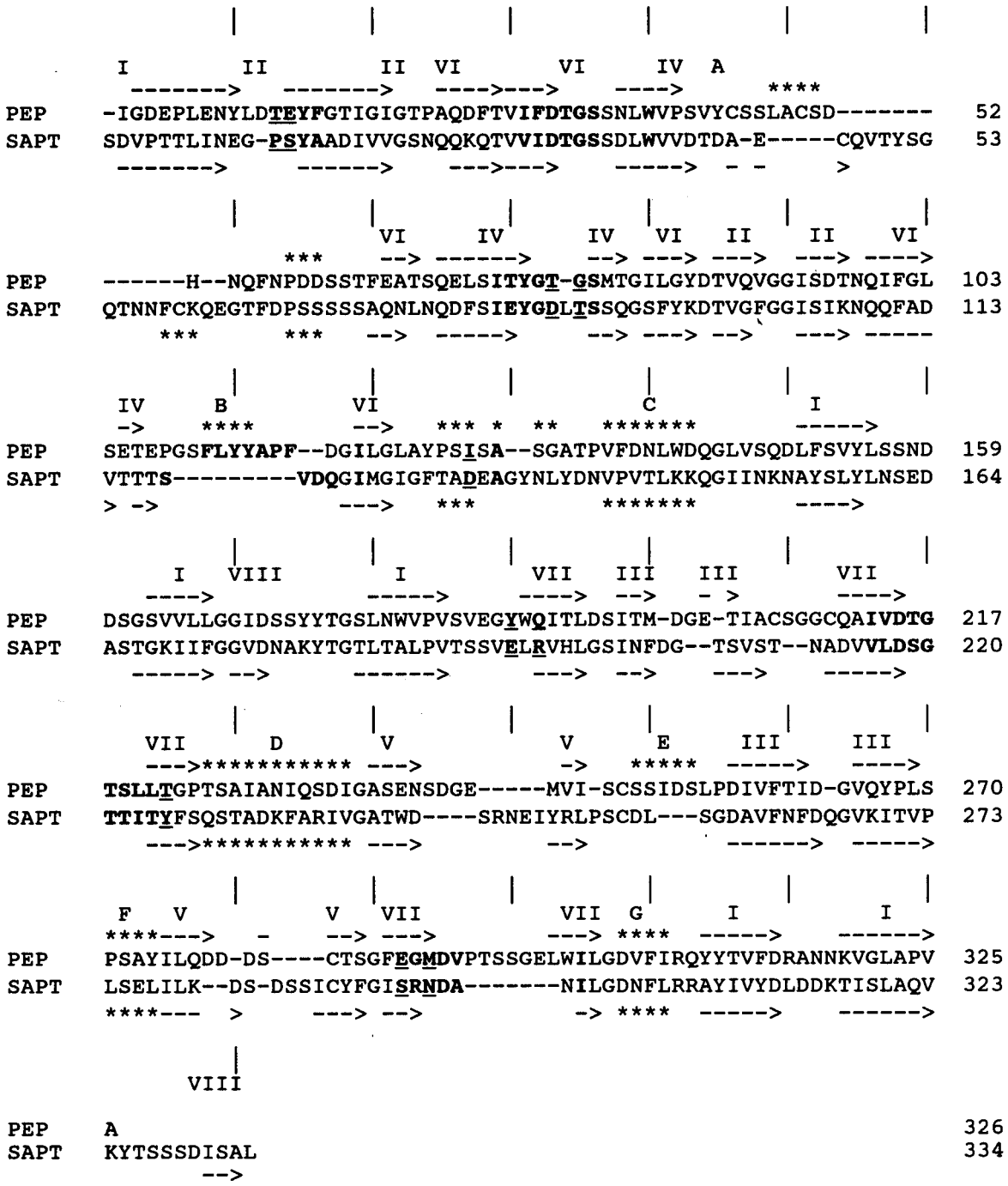

FIGURE 2: Structure-based sequence alignment between porcine pepsin (PEP) and *Candida tropicalis* aspartic proteinase (SAPT). Arrows indicate strands of β-sheet I−VIII. Asterisks indicate helix A−G or helical turn. Bold type indicates topologically equivalent residues of the SAPT binding cleft. Bold underlined type indicates residues which are topologically equivalent with important chemical differences.

observation that the enzyme has a loose substrate specificity when compared to other members of the aspartic proteinase family (Fusek *et al.*, 1994). During substrate−inhibitor binding, flexible loop 1 may compensate for the increased width of the cleft in a manner similar to that of the classic flap (James *et al.*, 1982), i.e. providing additional contacts with a ligand and shielding it from the solvent and thereby stabilizing the bound conformation. We hope to verify the role of the additional loop 1 through the analysis of SAPT complexes with inhibitors. On the primed side of the binding cleft, the differences between pepsin and SAPT are less obvious, with the exception of the shortened loop 3. This deletion may cause a loose substrate binding and specificity at position S_3'.

Like other aspartic proteinases, SAPT possesses the disulfide bridges at positions 45−50 and 249−282 (pepsin numbering). However, disulfide bridge 45−50 is not structurally conserved between pepsin and SAPT, and in SAPT, it anchors loop 1, which extends over the binding cleft. The second disulfide at position 249−282 is in the carboxyl-terminal subdomain. SAPT lacks the third disulfide bridge 201−206 which is observed in pepsin and the short surface loop associated with this part of the structure.

It is quite widely accepted that aspartic proteinases possess a mobile region positioned as the top of the carboxyl-terminal domain. In SAPT, this region consists of residues 198−215 and 226−294. On superimposing the Cα main chain atoms of the various aspartic proteinases to give a reasonable

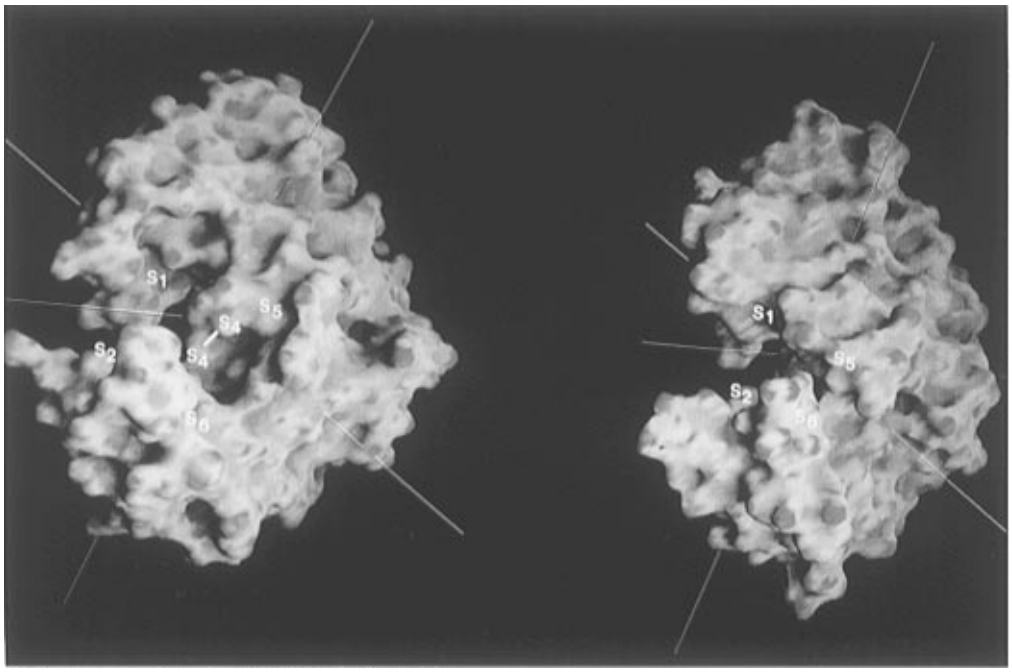

FIGURE 3: GRASP (Nichols *et al.,* 1991) rendering of the molecular surfaces of SAPT (left image) and porcine pepsin (right image) viewed in the direction of S_6-S_1 binding subsites. The labels indicate the equivalent binding regions of the two molecules. In SAPT, the S_4 site is wide, and beyond this binding region, the cleft diverges to form a deep canyon. The molecular surfaces were generated using the probe radius of 1.4 Å for both molecules.

Table 1: Relative Displacements of the Mobile Regions of Aspartic Proteinases versus SAPT[a]

	residues in least squares	rms deviation (Å)	no. of Cα pairs	rotation (deg)	trans. (Å)
pepsin	223−285	1.57	59	11.6	0.51
rhizopuspepsin	226−292	1.57	63	4.4	0.72
endothiapepsin	223−294	1.75	64	10.2	0.61
penicillopepsin	221−290	1.87	60	7.6	1.01

[a] In the first step of superposition, all Cα atoms from pairs of molecules were fitted using the algorithms LS_I and LS_E from the O program suite (Jones *et al.,* 1991). In the second stage of the analyses, the ranges of each mobile subdomain were defined by visualization of the overall pairwise superpositions. In the third step, the Cα atoms of the C-terminal subdomains were fitted and the relative displacements analyzed.

rms deviation of 1.5 Å, this region of the carboxyl-terminal lobe is found to systematically interfere with the overall fitting, despite its topological similarity with a corresponding target structure. When superimposed as a separate rigid body, the carboxyl-terminal region aligns significantly better. In pepsin, the region consists of residues 193−212 and 223−298 (Davies, 1990; Abad-Zapatero *et al.,* 1990). A similar region has also been observed in various conformations for other aspartic proteinases, for example in endothiapepsin complexed with peptidic inhibitors (Sali *et al.,* 1992) and in the zymogen form of pepsin, pepsinogen. For endothiapepsin, there are relatively few contacts between this region and the rest of the enzyme, and it deviates the greatest from pepsin. The function of the subdomain's mobility is not clearly understood. Apparently, it provides some flexibility to the binding cleft, and therefore, it should be considered during drug design. We have compared the SAPT structure with pepsin, rhizopuspepsin, endothiapepsin, and penicillopepsin and have found differences in the relative orientation of the carboxyl-terminal region as shown in Table 1. In our analysis, we observe that the rotational component of the rigid body motion is significantly larger than the translational component. An increased mobility of the SAPT area is indicated by the average temperature factor of 19.8 Å^2 relative to 15.2 Å^2 for the rest of the molecule. The SAPT carboxyl-terminal region's orientation is similar to fungal enzymes rhizopuspepsin and penicillopepsin but significantly differs from endothiapepsin and porcine pepsin as depicted in Figure 4.

In analyses of the early structures of aspartic proteinases, it was found that these enzymes have interdomain (Tang *et al.,* 1978) and intradomain (Blundell *et al.,* 1979) 2-fold symmetries. More recent studies have demonstrated that the interdomain symmetry is inexact in pepsin (Sielecki *et al.,* 1990) and other fungal aspartic proteinases (James & Sielecki, 1983; Suguna *et al.,* 1987a). Consistent with these findings in SAPT, we found 62 Cα atom pairs related by a 173° interdomain rotation with an rms deviation of 2.1 Å. The pseudo-dyad axis passes approximately between the catalytic aspartates D32 and D218 and the middle of β-sheet I. While the interdomain symmetry of aspartic proteinases may suggest an evolutionary distant gene duplication event followed by fusion and subsequent divergence etc., the prevailing asymmetry observed in these enzymes is consistent with the observations that inhibitors bind in one unique direction ($P_6 \rightarrow P_3'$).

Residual Density in the Active Site. A significant residual electron density was apparent close to the catalytic aspartates since the early stage of the refinement, with a shape strongly resembling a short peptide chain. Annealed omit maps (Hodel *et al.,* 1992) did not reveal any new features and did not suggest chemical bonding to any amino acid residue of the enzyme. An independently collected data set from a new crystal to 2.4 Å showed practically the same residual density and confirmed our initial observation. We applied a bulk solvent correction as implemented in the program X-PLOR (Brunger, 1992) and also solvent leveling using the model

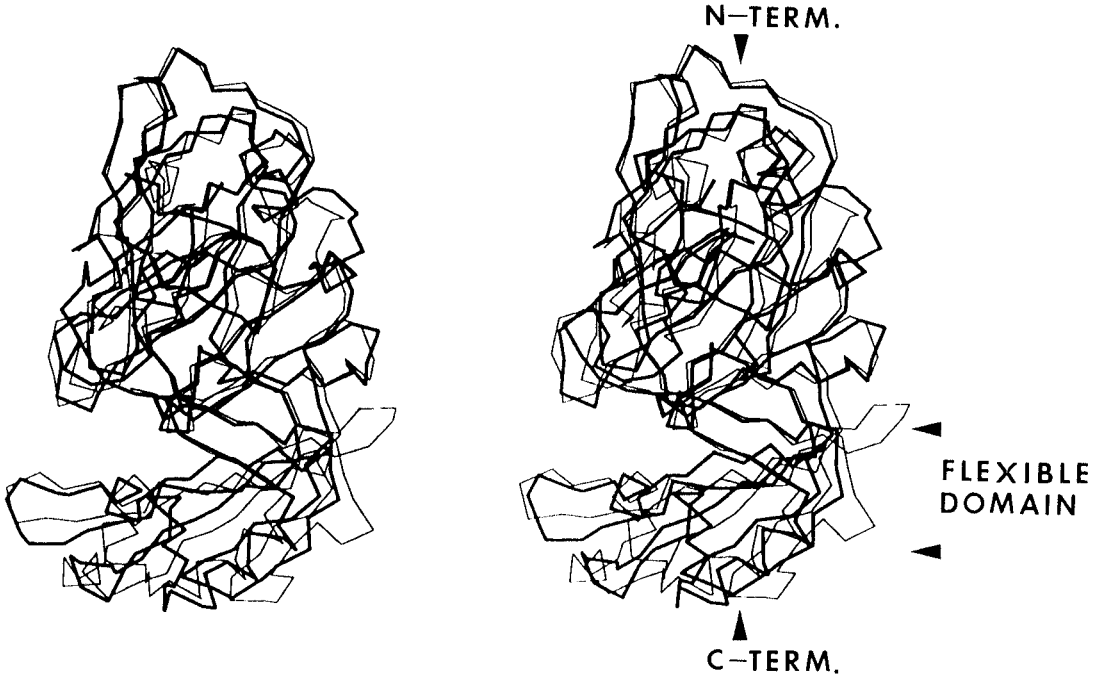

FIGURE 4: Stereoview of the Cα superposition of porcine pepsin (thin line) and SAPT (thick line) showing different orientations of the carboxyl-terminal subdomain. The superposition was performed using 302 equivalent Cα pairs giving an overall rms of 1.5 Å. The amino- and carboxyl-terminal domains are labeled with arrows, and the flexible region of the carboxyl domain that includes residues 198−215 and 226−294 is labeled by arrows as a flexible domain.

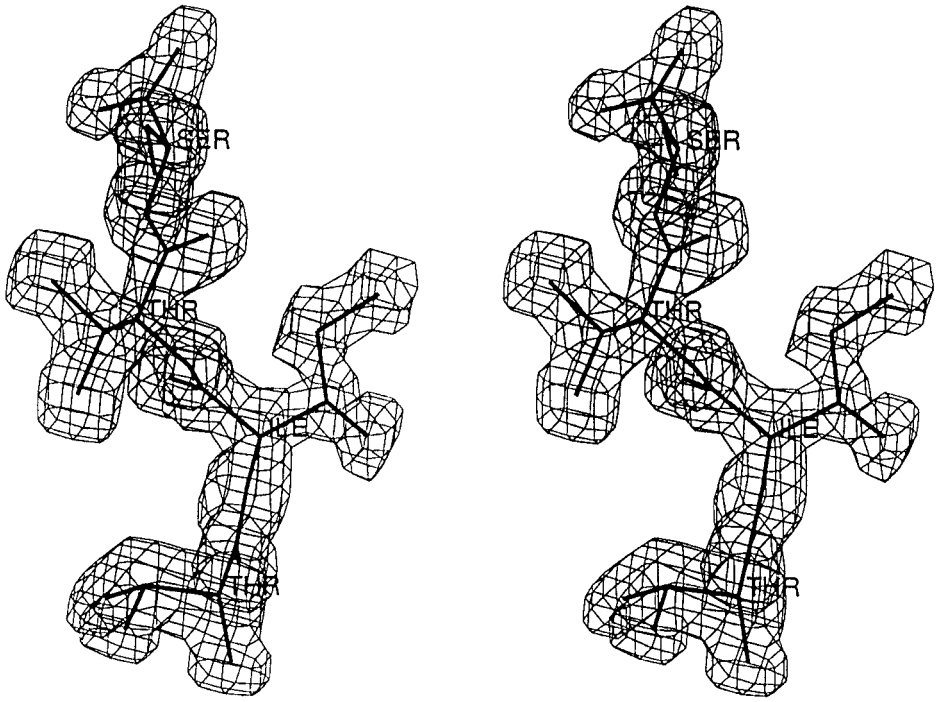

FIGURE 5: Stereoview of the $2F_o - F_c$ map at 1.8 Å resolution for the active site tetrapeptide with the model sequence Thr-Ile-Thr-Ser labeled at the Cα atoms.

mask in PHASES (Furey, 1989). Neither of these techniques showed any new features of the residual density. Before water molecules were added to the SAPT protein model, a tetrapeptide with the sequence $(Ala)_4$ was fitted to the residual density. The electron density map clearly defined the direction of the chain, which was consistent with expectations based on homologous inhibitor complexes.

Alternate amino acid sequences were fitted to the difference electron density in numerous cycles of simulated annealing refinement. The crystallographic sequencing efforts eventually led us describe the final sequence for the tetrapeptide as Xaa-Ile-Xaa-Ser, where Xaa is either Thr or Val. Figure 5 shows the final $2F_o - F_c$ electron density map for the tetrapeptide calculated at 1.8 Å resolution with the model sequence Thr-Ile-Thr-Ser. The electron density is clear and well-defined. The sequence Thr-Ile-Thr-Ser refined best with full occupancies and had an average temperature factor of 17.8 $Å^2$, which is similar to that for the whole protein molecule. The final $F_o - F_c$ map did not show any significant residual peaks around the assigned

sequence, suggesting that the tetrapeptide that is bound is restricted in its chemical structure.

A comparison with structures of endothiapepsin complexed with renin inhibitors (Foundling *et al.,* 1987) revealed that the peptide, which occupies SAPT binding sites $S_1'-S_3'$, matches the renin inhibitor main chain to within 0.5 Å. The tetrapeptide is bound in an extended conformation, making several hydrogen bonds and a number of nonbonded contacts with SAPT. We conclude from these comparisons that the interpretation of the residual density places the peptide in a credible position for binding in this enzyme. A symmetry-related SAPT molecule interacts with the carboxyl-terminal part of the tetrapeptide which would correspond to position P_4'. The steric hindrance of the symmetry mate is not severe; however, it does offer an alternative explanation for why the tetrapeptide is trapped in the crystal lattice rather than bound in the active site.

We attempted to elucidate the mechanism of formation, and the source, of the tetrapeptide found in the crystal structure. We have analyzed the full primary sequence of proSAPT for the possibility that the tetrapeptide is a cleavage peptide derived by autoproteolysis of the propart peptide from the proenzyme or from the mature enzyme itself. None of the sequences suggested by the crystallographic analysis can be found in the SAPT propart or in the mature SAPT enzyme sequence. The highly purified enzyme SAPT is fully active in solution, and we have concluded that SAPT will break down to intermediate-molecular weight fractions by autodigestion during incubation of a concentrated protein sample at room temperature (see Methods). However, SDS−PAGE analysis of the SAPT crystals has shown that autodigestion in the crystalline samples is negligible. The quality of the structure is also excellent, and the crystals diffract to high resolution which would suggest that the lattice is composed of a homogeneous population of molecules.

As a second possibility, we tested the hypothesis to determine whether any consistent tetrapeptide sequence could be located in the amino acid sequence of bovine serum albumin used in the *Candida* yeast fermentation. We could not identify the tetrapeptide in the BSA sequence. If this were the case, the tetrapeptide would likely copurify with SAPT during the column chromatography steps. This would require that it be tightly bound, and this would be manifest by low enzyme activity. When we tested activity with synthetic chromophoric peptide substrates which we have utilized in our studies on substrate specificity, the purified SAPT was determined to be highly active.

Third, we have not identified any protein cofactors from yeast which may copurify with SAPT, and SDS−PAGE gels of purifed SAPT indicate that our enzyme samples are homogeneous. It is possible that the tetrapeptide is an autodigestion product or is possibly a transpeptidation product (Antonov, 1985) cocrystallized with the full length SAPT enzyme.

Active Site, Binding Cleft, and Catalytic Mechanism. The molecular structure around the catalytic pair is the most highly conserved portion of aspartic proteinases. It characteristically has low thermal motion, is stabilized by an extensive network of hydrogen bonds (Davies, 1990), and is the most symmetric in terms of the interdomain pseudodyad axis.

Within each domain of aspartic proteinases, there is a structural motif that resembles the greek character ψ, located in β-sheets VI and VII of the amino-terminal and carboxyl-terminal domains, respectively. In this ψ-motif, the two outer β-strands are connected by a loop which crosses over the middle β-strand. This structure provides the underlying framework for the catalytic aspartates, which are located close to the ends of the connecting loops. In the SAPT molecule, chain segments V30−W39 and I123−G127 constitute ψ_1, and V216−Y225 and I298−N302 constitute ψ_2. The average temperature factors for ψ_1 and ψ_2 are 10.0 and 10.2 Å^2, respectively. Atomic superpositions for these ψ-motifs with the corresponding segments of pepsin, endothiapepsin, rhizopuspepsin, and penicillopepsin indicate high conservation, as the rms deviation does not exceed 0.54 Å for 30 equivalent Cα atom pairs.

Catalytic aspartates D32 and D128 of SAPT are found in the standard geometry about the local 2-fold axis. Their carboxyl groups are almost coplanar, and the shortest interatomic separation is 2.9 Å. There is also a hydrogen-bonded water molecule located between the two carboxyls in SAPT. This water is proposed to act as the nucleophile in the breaking of the peptide bond during catalysis in these enzymes (Suguna *et al.,* 1987b).

A new feature in the SAPT active site is the unexpected tetrapeptide which occupies the carboxyl-terminal side of the substrate binding cleft. The amino terminus of the tetrapeptide is within hydrogen bonding distance of both the water situated between the catalytic aspartates and of the carboxyl oxygen OD1 of aspartate D218. Figure 6 shows details of the active site with the tetrapeptide, and Table 2 gives the relevant hydrogen bond distances of the enzyme−peptide complex. There are three hydrogen bonds between the tetrapeptide and the SAPT binding cleft. The first interaction is between the amino-terminal nitrogen of the tetrapeptide and OD1, of aspartic D218, and two more interactions are made between backbone atoms of the tetrapeptide and the flap. Four hydrogen bonds are formed between the carboxyl-terminal S339 residue of the tetrapeptide and a symmetry-related SAPT molecule. There is an ionic interaction between the terminal carboxyl group of the tetrapeptide and the NZ of a K233 side chain from the symmetry-related molecule. There are seven hydrogen bonds between the tetrapeptide and water molecules. Five waters form part of a local network of hydrogen bonds between the enzyme and the peptide. All the other contacts are van der Waals interactions. Table 3 shows a distribution of nonbonding contacts less than 4.1 Å between the tetrapeptide and SAPT binding cleft, and the symmetry-related molecule. The majority of the contacts are to the binding site, especially at P_1'. A symmetry-related SAPT molecule binds to the P_4' position, thereby reducing its exposure to the bulk solvent.

The presence of the tetrapeptide could be due to two reasons. Either it is a chance interaction between the enzyme and a small peptide, or it is the result of cleavage by the enzyme on a longer peptide. However, in both cases, it exemplifies the position of binding for a possible cleavage product. If it is a cleavage product, then this aspartic proteinase ligand complex presented is the first to involve both a bound water between the catalytic pair and a bound ligand. In relation to the various catalytic mechanisms which have been proposed (Davies, 1990), we propose that the tetrapeptide in SAPT represents the final stage of product release, where the newly generated positively charged amino terminus of the substrate ($P_1' \rightarrow P_4'$) makes a favorable ionic

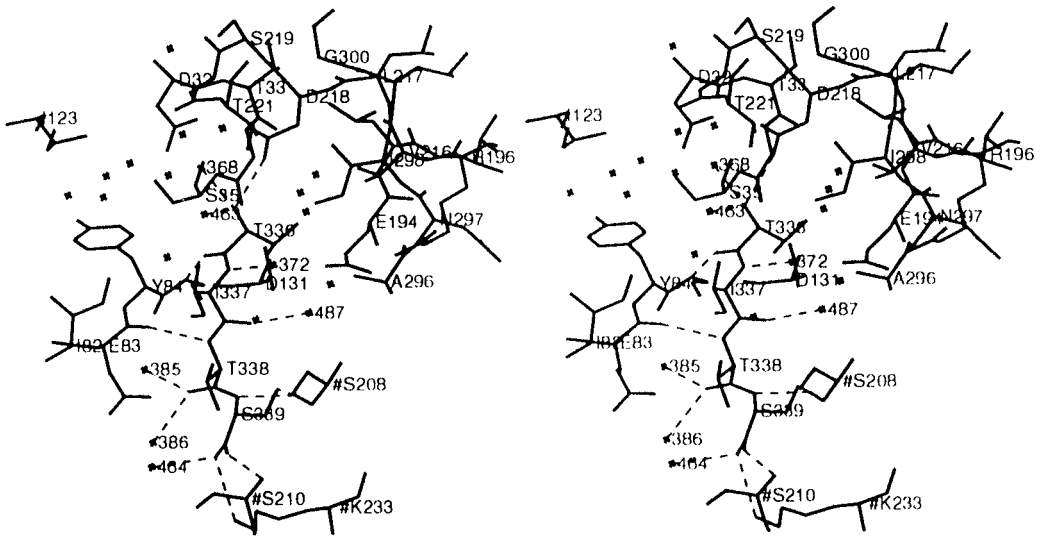

FIGURE 6: Stereoview of the active site with hydrogen bonds of the tetrapeptide Thr-Ile-Thr-Ser shown in dashed line. Water molecules are indicated by crosses. # indicates residues from a symmetry-related SAPT molecule.

Table 2: Hydrogen Bonds of the Tetrapeptide (Residues 336−339)[a]

donor	acceptor	distance (Å)
$T336_{N-term}$	$D218_{OD1}$	2.80
$G85_N$	$T336_O$	2.80
$T338_N$	$E83_O$	2.96
$S339_N$	$S208_O$[b]	2.99
$S339_{OG1}$	$S208_O$[b]	3.23
$S210_N$[b]	$S339_{OT1}$	2.74
$K233_{NZ}$[b]	$S339_{OT2}$	3.18
$T336_N$	$WAT368_O$	2.68
$T336_N$	$WAT463_O$	2.85
$I337_N$	$WAT372_O$	2.86
$WAT487_O$	$I337_O$	2.80
$WAT385_O$	$T338_O$	2.85
$WAT464_O$	$S339_{OT2}$	3.09
$WAT386_O$	$T338_O$	3.20

[a] An H bond cutoff distance of 3.5 Å was applied. Donor/acceptor code: single-letter amino acid code, residue number, and atom label. WAT = water molecule. [b] Symmetry mate molecule $-x + 1$, $y + 0.5$, and $-z + 0.5$.

Table 3: Distribution of Nonbonded Contacts Less Than 4.1 Å from the Tetrapeptide Thr-Ile-Thr-Ser

	P_1'	P_2'	P_3'	P_4'
no. of contacts with SAPT binding site	20	11	9	0
no. of contacts with symmetry mate	0	1	5	16

interaction with a negatively charged OD1 of D218. The amino-terminal portion of the substrate ($P_6 \rightarrow P_1$) has been released from the binding cleft, and the catalytic water has reoccupied the central position between the two catalytic aspartates, thus facilitating another round of catalysis in the enzyme. Our observation that the tetrapeptide cleavage product occupies binding subsites $S_1' \rightarrow S_3'$ in SAPT is unique for this class of enzymes, and it suggests that the amino-terminal cleavage fragment leaves before the carboxyl-terminal fragment.

Several differences in local structure are observed in the comparison of the pepsin and SAPT binding clefts. The first profound difference likely to alter the substrate specificity is the deletion of helix B (Figure 2). In pepsin, this region is predominantly hydrophobic. In SAPT, the shorter and more polar segment SVDQ, which is 3.5 Å closer to the catalytic pair, may influence the substrate preference in the

Table 4: Proposed SAPT Binding Subsites[a]

S_5	S_4	S_3	S_2	S_1	S_1'	S_2'	S_3'
$P12_M$	$P12_M$	$P12_M$	$G85_M$	$V30_S$	$G34_M$	$S35_{M/S}$	$E83_S$
$Y51_S$	$T222_S$	$S13_{M/S}$	$D86_{M/S}$	$D32_S$	$G85_M$	$I82_S$	$G85_M$
$D120_S$	$I223_S$	$D86_S$	$T221_S$	$S35_{M/S}$	$E194_S$	$E83_S$	
	$Y225_S$	$T88_{M/S}$	$Y225_S$	$Y84_S$	$R196_S$	$Y84_S$	
	$I248_S$	$D120_S$	$N294_S$	$D86_{M/S}$	$V216_S$	$D131_S$	
	$L279_S$	$T222_S$	$A296_S$	$T88_S$	$D218_S$	$A133_S$	
			$I298_S$	$V119_S$	$A296_S$		
				$I123_S$	$I298_S$		
				$G220_M$			

[a] The enzyme subsite definition S_5-S_3' of Schechter and Berger is used. $Residue_M$ indicates main chain predominant contact. $Residue_S$ indicates side chain predominant contact. $Residue_{M/S}$ indicates that main and side chain contribute equally to contact.

binding subsites S_1 and S_3. A second notable change is in the β-turn at pepsin numbering L10-D11-T12. SAPT forms a simpler, more restricted β-turn at G11−P12 which modifies binding subsites S_3-S_5. The third difference is the orientation of the carboxyl-terminal region. This difference is expected to influence binding at subsite S_6 and, to a lesser extent, subsite S_4. The fourth structural difference is found on the carboxyl-terminal side of the binding cleft ($S_1'-S_3'$). In pepsin, loop 290−297 may potentially interact with residues occupying S_3'. SAPT lacks this local structure, and the cleft is therefore more exposed. Finally, it is interesting to note the insertion of L87 in the β-turn of the SAPT flap. This turn is different from that of pepsin, but it is structurally homologous to endothiapepsin, rhizopuspepsin, and penicillopepsin, all of which have a glycine at this position.

On the basis of structural comparisons with pepsin−inhibitor complexes (Abad-Zapatero *et al.*, 1991), we have identified 43 residues that we propose are involved in substrate−inhibitor binding in SAPT (Figure 2 and Table 4). There are no distinct boundaries between the binding subsites, but this traditional subdivision assists in the description of the binding cleft. Thirty-one of the 43 residues identified are conserved or conservatively varied between pepsin and SAPT. We have identified 10 topologically equivalent residues that are significantly different in their chemical properties and so are likely to influence the substrate−inhibitor specificity of SAPT (Figure 2).

Table 5: SAPT Diffraction Data and Refinement Statistics

	data set 1	data set 2[a]
no. of crystals	3	1
no. of observed reflections	215 435	63 030
no. of unique reflections	32 636	20 300
R_{sym}[b] (%)	6.8	3.8
refinement resolution (Å)	8.0−1.8	8.0−2.4
no. of $F > 2\sigma_F$	28 918	11 555
completeness (%)[c]	93	88
no. of amino acids[b]	338	334
no. of water molecules	231	
no. of ethanol molecules	6	
R-factor[e] (%)	18.3	
R-factor for all data (%)	22.6	
rms[f] for bonds (Å)	0.011	
rms for angles (deg)	1.764	
Luzzati (Luzatti, 1952) coordinate error (Å)	0.19	
average *B* for protein (Å^2)	16.6	

[a] Used for a check map calculation only. [b] $R_{sym} = \langle|I - \langle I\rangle|/|\langle I\rangle|\rangle$, where $\langle I\rangle$ is an average of all observations of the reflection. [c] In the data resolution range of 40−1.8 Å, we collected 30 348 observed reflections of a possible total of 31 594$_{CALC}$ to give 96.1% completeness. In the highest-resolution data shell of 1.92−1.80 Å, the percentage observed is 91.4% complete. [d] There are 334 amino acid residues of the protein + four residues of the peptide. [e] $R = \sum||F_o| - |F_c||/\sum|F_o|$. [f] rms = root mean square deviation.

One of the most significant amino acid changes is at pepsin position T77 → D(86)$_{SAPT\ NUMBERING}$. D(86) is located at the tip of the flap in SAPT, which is typical of the fungal aspartic proteinases. The side chain is projected down, in a hooklike conformation into the binding cleft, and potentially interacts with substrate residues occupying the S_1−S_3 binding subsites. Two significant changes are found at positions Y189 → E(194) and I128 → D(131), which may influence the substrate specificity at the cleft subsites S_1' and S_2'.

In general, the structure of SAPT has revealed that the more spacious binding cleft has more charged amino acids D/E and R when compared to pepsin which is more hydrophobic and neutral in character (Sielecki *et al.,* 1990). We hope to extend the structural studies of SAPT with additional analyses of enzyme−inhibitor complexes and verify some of our projections of substrate specificity in the SAPT molecule.

DISCUSSION

Substrate Specificity. The detailed three-dimensional model of the *C. tropicalis* enzyme presented here has been compared with other crystallographically solved aspartic proteinases and complexes with inhibitors (Foundling *et al.,* 1987; Blundell *et al.,* 1987; Fraser *et al.,* 1992; Greenlee, 1990; Ocain & Abou-Gharbia, 1991; Petteway *et al.,* 1991; Bailey & Cooper, 1994). These comparisons have assisted us in the definition of the substrate specificity.

One such structural comparison is shown in Figure 7. The structural alignment was obtained using the Kabsch algorithm implemented in the program ALIGN (Satow *et al.,* 1986). The Cα atoms of the SAP2X *C. albicans* enzyme (Abad-Zapatero *et al.,* 1996) were used to fit against the Cα atoms of the SAPT enzyme. The resulting fit gave a rms deviation of 1.14 Å for 332 atom pairs, with a maximum deviation of 2.95 Å. This placed the inhibitor A-70450 of the SAP2X structure into the active site cleft of the SAPT, and several close nonbonded contacts were observed between the inhibitor and the enzyme. One particularly close contact was observed between position S_2 of A-70450 and D86 of the flap. By comparison, the superposition of Cα atoms of a rhizopuspepsin−inhibitor complex onto the SAPT structure (1apr; Suguna *et al.,* 1987b) gave a rms deviation of 2.47 Å for 247 Cα pairs, with a maximum deviation of 9.71 Å. The reduced bond inhibitor of the rhizopuspepsin complex could not easily be accommodated into the cleft of SAPT enzyme, due to steric hindrance. The *Candida* enzymes, including the SAPT enzyme, have specific features which classify this group as moderately divergent from fungal enzymes (Bailey & Cooper, 1994; Abad-Zapatero *et al.,* 1996).

We have used these modeling studies, together with a further evaluation of our earlier substrate specificity screening of three secreted *Candida* enzymes (Fusek *et al.,* 1994), to probe the SAPT enzyme for indications of substrate specificity. This analysis demonstrated that the specificity of the *Candida* enzymes is broad and similar to the cleavage specificities observed for other fungal enzymes and gastric enzymes (Fruton, 1976). In addition, it has been demonstrated that the recombinant *C. tropicalis* enzyme can process its own propart sequence from the zymogen precursor, to generate the mature enzyme which requires a cleavage at an Arg−Ser bond. This is an unusual substrate specificity for an aspartic proteinase. In addition to this major cleavage, proSAPT was also observed to cleave the adjacent bonds Lys−Arg and Gln−Lys of the SAPT propart sequence (Lin *et al.,* 1993).

From our combined observations, a generalization can be made with respect to the binding specificities for SAPT. Aspartic proteinases in general show a strong preference for a sequence with hydrophobic side chains at positions P_1 and P_1' in a substrate (Hsu *et al.,* 1976; Fruton, 1971). In SAPT, the S_1 binding subsite has predominantly hydrophobic residues V30, V119, and I123, and an aromatic Y84. Two additional residues of the flap, D86 and T88, are specificity determinants in the S_1 environment (Lowther *et al.,* 1995). An exception to this usual cleavage specificity was observed in analyses of the recombinant proSAPT. This is probably due to the close proximity of D86 conferring the specificity for cleavage adjacent to a positively charged residue.

The specificity screening experiments indicated a preference for a hydrophobic Leu, or longer positive side chain of Lys or Arg in position P_2. Substrates with either Asp or Glu at P_2 caused low catalytic cleavage rates to be observed. The latter could also have been due to the presence of D86 at the flap. The residues that form the S_2 environment are a mixture of neutral, polar, and hydrophobic residues: G85, T221, Y225, N294, and I298. The S_2 environment is solvent-accessible, and the longer side chains of Lys and Arg of a substrate can be easily accommodated with the potential to stabilize a positive charge through solvation.

The S_3 subsite environment is predominantly polar and negatively charged. This is unusual for an aspartic proteinase. SAPT was found to reject an Asp at the P_3 position. Residues D120 and possibly D86 are the likely candidates for eliciting this specificity. In the three-dimensional structure, it is apparent that the S_3 binding site is cavernous, and may thus be able to accommodate a wide variety of residues except for negatively charged ones.

The S_4 binding environment was found to disallow Leu at P_4. This is difficult to explain since the subsite is relatively open. It is possible that the bulky Y225 restricts space in the S_4 environment. Another possible explanation for the

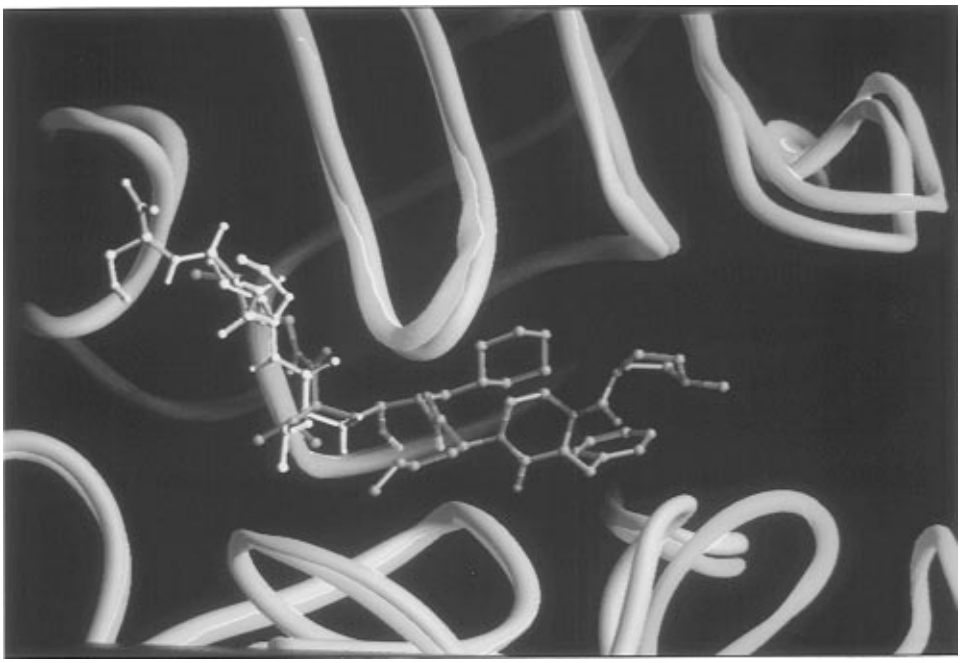

FIGURE 7: Comparison of the folding of SAPT (cyan ribbon image) and SAP2X (gold ribbon image). The Abbott inhibitor A-70450 (green ball and stick) and SAPT tetrapeptide (magenta ball and stick) are shown occupying the active site cleft.

restrictive specificity may come from the observed mobility of the carboxyl-terminal region. A rigid-body shift in this region may significantly alter the shape of the S_4 subsite and restrict the size accommodated in S_4. The S_5 subsite is considerably wider than S_4 and can likely accommodate a broad variety of residues at position P_5. In our analysis of specificity, this was the last position tested with two variations of Lys or Arg at the amino terminus of substrates.

The length of substrate recognized C-terminal to the scissile bond is significantly shorter than on the N-terminal side. Generally, subsites S_1' and S_2' bind substrate−inhibitor residues tightly; however, at S_3', the binding is loose and a P_3' residue makes very few contacts with the enzyme (Bailey & Cooper, 1994). The primary specificity subsite S_1' is relatively exposed and evidently charged, with a Glu at position 194 and Arg at 196. These two charged residues may confer the recombinant SAPT with the ability to bind the propart peptide to facilitate autoactivation, primarily at the Arg−Ser bond (of propart), but also at a minor cleavage site, the adjacent Lys−Arg bond. Our substrate specificity analysis did not investigate modifications in this position. At S_2', we found that each substitution made to replace the P_2' Arg lowered initial cleavage velocities with SAPT. An Arg side chain can adopt several different conformations in the S_2' region from our modeling studies and maintain stability in interacting with the enzyme.

The principle S_2' residues are I82, D131 and A133. It is likely that the D131 residue is responsible for strongly rejecting a P_2' Asp in substrate. The selectivity of the S_3' site was not investigated; however, we do not expect it to show a restrictive specificity. S_3' is solvent-exposed. The number of contacts offered by the enzyme are limited to two residues in the vicinity of S_3'; they are E83 and G85. Changing to a positive residue may be more favorable at P_3'.

In conclusion, this is the first monomeric aspartic proteinase complex published, where a clearly defined substrate portion has been captured at the active site. Further structural studies on complexes of *C. tropicalis* SAPT with inhibitors or substrate analogues are needed to elucidate the mode of binding to the full active site cleft.

ACKNOWLEDGMENT

We thank Dr. Cele Abad-Zapatero of Abbott Research Laboratories for providing us with a SAP2X model of his *C. albicans* enzyme prior to publication. We thank Dr. M. Fusek for help with protein purification and crystal growth. We acknowledge the help of Dr. A. C. Treharne in proofreading the manuscript.

REFERENCES

Abad-Zapatero, C., Rydel, T. J., & Erickson, J. (1990) *Proteins: Struct., Funct., Genet. 8*, 62−81.

Abad-Zapatero, C., Rydel, T. J., Neidhart, D. J., Luly, J., & Erickson, J. W. (1991) in *Structure and Function of the Aspartic Proteinases* (Dunn, B. M., Ed.) pp 9−21, Plenum Press, New York.

Abad-Zapatero, C., Goldman, R., Muchmore, S. W., Hutchins, C., Stewart, K., Navaza, J., Payne, C. D., & Ray, T. L. (1996) *Protein Sci. 5*, 640−652.

Andreeva, N. S., Fedorov, A. A., Gustchina, A. E., Riskulov, R. R., Safro, M. G., & Shutzkever, N. E. (1978) *Mol. Biol. (Engl. Transl.) 12*, 704−707.

Antonov, V. K. (1985) in *Aspartic Proteinases and their Inhibitors* (Kostka, V., Ed.) pp 203−220, Walter de Gruyter & Co., Hawthorne, NY.

Bailey, D., & Cooper, J. (1994) *Protein Sci. 3*, 2129−2143.

Blum, J. S., Fiani, M. L., & Stahl, P. D. (1991) in *Structure and Function of the Aspartic Proteinases: Genetics, Structures and Mechanisms* (Dunn, B. M., Ed.) pp 281−289, Plenum Press, New York.

Blundell, T. L., Sewell, B. T., & McLachlan, A. D. (1979) *Biochim. Biophys. Acta 580*, 24−31.

Blundell, T. L., Cooper, J., Foundling, S. I., Jones, D. M., Atrash, B. & Szelke, M. (1987) *Biochemistry 26*, 5585−5590.

Borg, M., & Rüchel, R. (1990) *J. Med. Vet. Mycol. 28*, 3−14.

Brunger, A. T. (1992) *X-PLOR Manual*, Version 3.1, Yale University Press, New Haven, CT.

Calderone, R. A., & Stevens, D. A. (1991) *Microbiol. Rev. 55*, 1−20.

Carson, M. (1997) *RIBBONS, Methods Enzymol.* (in press).
Chen, K. C. S., & Tang, J. (1972) *J. Biol. Chem. 247*, 2566−2574.
Chothia, C., & Janin, J. (1982) *Biochemistry 21*, 3955−3965.
Cooper, J. B., Kahn, G., Taylor, G., Tickle, I. J., & Blundell, T. L. (1990) *J. Mol. Biol. 214*, 199−222.
Cutfield, S. M., Dodson, E. J., Anderson, B. F., Moody, P. C. E., Marshall, C. J., Sullivan, P. A., & Cutfield, J. F. (1995) *Structure 3*, 1261−1271.
Cutler, J. E. (1991) *Annu. Rev. Microbiol. 45*, 187−218.
Davies, D. R. (1990) *Annu. Rev. Biophys. Chem. 19*, 189−215.
Debouck, C., & Metcalf, B. W. (1990) *Drug Dev. Res. 21*, 1−17.
Dreyer, T., Halkjaer, B., Svenden, I., & Otterson, M. (1985) in *Aspartic Proteinases and their Inhibitors* (Kostka, V., Ed.) pp 41−44, Walter de Gruyter & Co., Hawthorne, NY.
DuPont, B., Denning, D. W., Marriott, D., Sugar, A., Viviani, M. A., & Sirisanthana, T. (1994) *J. Med. Vet. Mycol. 32* (Suppl. 1), 65−77.
Foltmann, B. (1981) *Essays Biochem. 17*, 52−84.
Foundling, S. I., Cooper, J., Watson, F. E., Cleasby, A., Pearl, L. H., Sibanda, B. L., Hemmings, A., Wood, S. P., Blundell, T. L., Valler, M. J., Norey, C. G., Kay, J., Boger, J., Dunn, B. M., Leckie, B. J., Jones, D. M., Atrash, B., Hallett, A., & Szelke, M. (1987) *Nature 327*, 349−352.
Fraser, M. E., Strynadka, N. C. J., Bartlett, P. A., Hanson, J. E., & James, M. N. G. (1992) *Biochemistry 31*, 5201−5214.
Fruton, J. S. (1971) in *The Enzymes* (Boyer, P., Ed.) Vol. 3, pp 120−164, Academic Press Inc.
Fruton, J. S. (1976) *Adv. Enzymol. Relat. Areas Mol. Biol. 44*, 1−33.
Furey, W. (1989) *PHASES*, University of Pittsburgh, Pittsburgh, PA.
Fusek, M., Smith, E. A., Monod, M., Dunn, B. M., & Foundling, S. I. (1994) *Biochemistry 33*, 9791−9799.
Greenlee, W. J. (1990) *Med. Res. Rev. 10*, 173−186.
Hodel, A., Kim, S.-H., & Brunger, A. T. (1992) *Acta Crystallogr. A 48*, 851−858.
Hsu, I.-N., Hofmann, T., Nyburg, S. C., & James, M. N. G. (1976) *Biochem. Biophys. Res. Com. 72*, 363−368.
James, M. N. G., & Sielecki, A. R. (1983) *J. Mol. Biol. 163*, 299−361.
James, M. N. G., Sielecki, A., Salituro, F., Rich, D. H., & Hofmann, T. (1982) *Proc. Natl. Acad. Sci. U.S.A. 79*, 6137−6141.
Jones, T. A., Zou, J. Y., Cowan, S. W., & Kjeldgaar,d M. (1991) *Acta Crystallogr. A 47*, 110−119.
Kay, J., Valler, M. J., Keilova, H., & Kostka, V. (1981) in *Proteinases and their Inhibitors* (Turk, V., Ed.) pp 1−17, Walter de Gruyter and Co., Hawthorne, NY.
Knowles, J. R. (1970) *Philos. Trans. R. Soc. London, Ser. B B257*, 269−277.
Laskowski, R. A., MacArthur, M. W., Moss, D. S., & Thornton, J. M. (1993) PROCHECK *J. Appl. Crystallogr. 26*, 283−291.
Lin, X. L., Tang, J., Koelsch, G., Monod, M., & Foundling, S. I. (1993) *J. Biol. Chem. 268*, 20143−20147.
Lowther, W. T., Majer, P., & Dunn, B. M. (1995) *Protein Sci. 4*, 689−702.
Luzatti, V. (1952) *Acta Crystallogr. 5*, 802−810.
MacDonald, F., & Odds, F. C. (1980) *J. Med. Microbiol. 13*, 423−435.
Metcalf, P., & Fusek, M. (1993) *EMBO J. 12*, 1293−1302.
Morihara, K. (1973) *Adv. Enzymol. 41*, 179−243.
Navaza, J. (1994) AMoRe, *Acta Crystallogr. A 50*, 157−163.
Nicholls, A., Sharp, K. A., & Honig, B. (1991) *Proteins: Struct., Funct., Genet. 11*, 281−296.
Ocain, T. D., & Abou-Gharbia, M. (1991) *Drugs Future 16*, 37−51.
Odds, F. C. (1994) *J. Am. Acad. Dermatol. 31*, 2−5.
Petteway, S. R., Jr., Dreyer, G. B., Meek, T. D., Metcalf, B. W., & Lamber, D. M. (1991) *AIDS Res. Rev. 1*, 267−288.
Ray, T. L., & Payne, C. D. (1987) *Clin. Res. 35*, 711A.
Ray, T. L., & Payne, C. D. (1988) *Infect. Immun. 56*, 1942−1949.
Rüchel, R., Boning-Stutzer, B., & Mari, A. (1988) *Mycoses 31*, 87−106.
Rüchel, R., Zimmermann, F., Boning-Stutzer, B., & Helman, U. (1991) *Virchows Arch. A: Pathol. Anat. Histopathol. 419*, 199−202.
Rüchel, R., De Bernardis, F., Ray, T. L., Sullivan, P. A., & Cole, G. T. (1992) *J. Med. Vet. Mycol. 30*, (Suppl. 1), 123−132.
Sack, J. S. (1998) *J. Mol. Graphics 6*, 224−225.
Sali, A., Veerapandian, B., Cooper, J. B., Moss, D. S., Hofmann, T., & Blundell, T. L. (1992) *Proteins: Struct., Funct., Genet. 12*, 158−170.
Sardinas, J. L. (1965) *Appl. Microbiol. 166*, 248−263.
Satow, Y., Cohen, G. H., Padlan, E. A.& Davies, D. R. (1986) *J. Mol. Biol. 190*, 593−604.
Schechter, I., & Berger, A. (1970) *Biochem. Biophys. Res. Commun. 2*, 157−162.
Shewale, J. G., Takahashi, T., & Tang, J. (1985) in *Aspartic Proteinases and their Inhibitors* (Kostka, V., Ed.) pp 101−116, Walter de Gruyter & Co., Hawthorne, NY.
Sielecki, A. R., Fedorov, A. A., Boodhoo, A., Andreeva, N. S., & James, M. N. G. (1990) *J. Mol. Biol. 214*, 143−170.
Siemens Analytical X-ray Instruments (1989) *FRAMBO, SADIE, SAINT*, 6300 Enterprise Lane, Madison, WI 53719.
Subramanian, E., Swan, I. D. A., & Davies, D. R. (1976) *Biochem. Biophys. Res. Commun. 68*, 875−880.
Suguna, K., Bott, R. R., Padlan, E. A., Subramanian, E., Sheriff, S., Cohen, G. H., & Davies, D. R. (1987a) *J. Mol. Biol. 196*, 877−900.
Suguna, K., Padlan, E. A., Smith, C. W., Carlson, W. D., & Davies, D. R. (1987b) *Proc. Natl. Acad. Sci. U.S.A. 84*, 7009−7013.
Swartz, M. N. (1994) *Proc. Natl. Acad. Sci. U.S.A. 91*, 2420−2427.
Tang, J., Sepulveda, P., Marciniszyn, J., Chen, K. C. S., Huang, W.-Y., Tao, N., Liu, D., & Lanier, S. P. (1973) *Proc. Natl. Acad. Sci. U.S.A. 70*, 3437−3439.
Tang, J., James, M. N. G., Hsu, I. N., Jenkins, J. A., & Blundell, T. L. (1978) *Nature 271*, 618−621.
Togni, G., Sanglard, D., Falchetto, R., & Monod, M. (1991) *FEBS Lett. 286*, 181−185.
Wlodawer, A., Miller, M., Jaskolski, M., Sathyanarayana, B. K., Baldwin, E., Weber, I. T., Selk, L. M., Clawson, L., Schneider, J., & Kent, S. B. H. (1989) *Science 245*, 616−621.

BI970613X